Analysis of Adhesive-Free Bonding Performance of Poplar Wood Surface Swelled with NaOH Solution

Xinming Wang, Xudong Zhu, and Liang Qian *

Poplar wood specimens were fabricated *via* surface swelling pretreatment with NaOH solution combined with a hot-pressing process. The three factors NaOH concentration, hot-pressing temperature, and hot-pressing time were considered relative to shear strength. The optimal process parameters for poplar adhesive-free bonding were surface swelling with 5% NaOH solution, a hot-pressing temperature of 140 ºC, and a hot-pressing time of 60 min. Under these parameters, the shear strength of the prepared specimens' bonding interface reached 4.87 MPa. Analysis of variance showed that hot-pressing temperature exerted a highly significant effect on shear strength and that temperature was the dominant factor influencing adhesive-free bonding performance. Scanning electron microscopy observations indicated that NaOH solution surface swelling had a notable impact on the adhesive boundary, facilitating the formation of a dense adhesive layer in this area. Furthermore, a distinct phenomenon of molten lignin encapsulating fibers was observed at the bonding interface. As a natural bonding medium, molten lignin effectively enhances the bonding between fibers, thereby improving the adhesive-free bonding strength of poplar wood. Hemicellulose underwent substantial degradation, while no significant degradation was observed in the skeletal structure of lignin. This study provides a theoretical foundation and technical reference for optimizing the poplar wood adhesive-free bonding process.

DOI: 10.15376/biores.21.4.9541-9554

Keywords: Adhesive-free; Wood; Shear strength

Contact information: Yangzhou Polytechnic Institute, Jiangsu 225100, China;
** Corresponding author:50908912@qq.com*

INTRODUCTION

Wood, bamboo, and their composites are crucial raw materials in furniture manufacturing and construction engineering. In traditional production, adhesives containing urea-formaldehyde and phenolic resin are commonly used to prepare engineered wood. In recent years, the application of alkaline pretreatment in the modification of wood-based materials has garnered widespread attention from researchers. This technology involves pretreating wood and bamboo with alkaline reagents such as sodium hydroxide (NaOH), sodium sulfite (Na_2SO_3), sodium hypochlorite (NaClO), and sodium chlorite ($NaClO_2$). And then the pretreating wood and bamboo was used to produce high-strength products by hot pressing (Qian *et al*. 2024). Related research focuses on optimizing the alkali-based treatment process and reaction conditions, aiming to enhance the wood modification effect and material mechanical properties, thereby improving the utilization rate of wood resources and providing a feasible technical path for the development of high-performance glue-free wood-based materials.

Andze *et al.* (2026) successfully prepared high-performance wood-based materials by pretreating wood with 1 M sodium hydroxide at 145 ℃ for 10 to 30 min, combined with radial compression densification process. Research by Qiu (2025) further revealed the evolution of microstructure. It was found that as the NaOH treatment time increased from 1.0 h to 12 h, the cellular structure of wood gradually collapsed and reorganized into a wavy porous structure, significantly increasing the specific surface area and porosity. This promotes the expansion and openness of the wood's pore structure and thus enhancing the adsorption performance of the material. In terms of process optimization, Zheng *et al*. (2025) addressed the permeability issue of *Eucalyptus urophylla* by impregnating it with a mixture of NaOH and Na_2SO_3, determining the optimal process as 5% NaOH and 3 h of immersion time, which increased the water absorption percentage of wood from 29.0% to 60.0%, and the porosity from 31.8% to 42.8%. Wang *et al*. (2026) modified camphor wood using dilute alkali solution. Liu (2025) treated fast-growing poplar veneer with NaOH/H_2O_2 synergistic modification, resulting in an increase in surface micron-scale concave-convex structure and roughness, showing better interfacial bonding potential. In addition, Qi *et al*. (2023) confirmed that using NaOH as a pretreatment agent can effectively improve the dye absorption rate of Chinese fir, white oak, and poplar wood. In summary, using alkali solutions such as NaOH for treatment has become an effective means for efficient utilization of wood, helping to form substrates with three-dimensional networks and porous structures (Wu *et al*. 2020; Yang *et al*. 2020; Zhao *et al*. 2021; Wang *et al*. 2023), laying a solid foundation for the preparation of high-performance composite materials.

Research has confirmed that treating wood with a mixed solution of NaOH and Na_2SO_3 not only effectively removes lignin and hemicellulose but also enhances ethanol production, providing important technical support for the modification and high-value utilization of wood-based materials (Fan *et al*. 2020; Pang *et al*. 2021). In terms of the preparation of cellulose-based and densified materials, Song *et al.* (2018) obtained dense wood by immersing natural wood in a boiling solution of 2.5 M NaOH and 0.4 M Na_2SO_3 for 7 h, followed by hot pressing at 100 ℃ and 5 MPa for 1 day. Chen *et al*. (2018) prepared wood carbon sponges using the same mixed alkali solution and soaking process. Xu *et al*. (2019) boiled wood samples in a mixed solution of 2 M NaOH and 0.5 M Na_2SO_3 for 4 h, followed by treatment with a 2 M H_2O_2 solution for 5 h, successfully preparing highly compressible cellulose-based materials, expanding the application scenarios of alkali-treated wood. In terms of improving ethanol yield from wood and developing functional materials, Ye *et al*. (2023) soaked pine wood chips in a solution of 2 M NaOH and 0.4 M Na_2SO_3, stirred, and heated at 96 ℃ for 4 h, successfully developing a wood-based functional material. Bay *et al*. (2020) pretreated wood with a mixed solution of NaOH and Na_2CO_3, significantly improving ethanol yield.

Currently, various delignification methods based on chlorine-based reagents and alkaline solutions have been developed in the scientific research field, and the relevant research results have provided important support for the modification and application of wood-based materials. The core driving force of the delignification process is the oxidizing effect of chlorine (ClO_2) radicals, which breaks the aromatic rings in lignin, thereby achieving efficient decomposition and removal of lignin (Yang *et al*. 2023). Jungstedt *et al*. (2020) prepared a 1.0 wt% NaClO solution using acetic acid buffer, fully immersed the wood, and controlled the treatment temperature to be stable at 80 ℃, successfully achieving delignification of wood. Hu *et al*. (2023) adopted a similar treatment scheme in their research, further verifying the feasibility of this method. In addition, Mi *et al*. (2019)

selected balsa wood as the raw material in the preparation process of transparent wood, effectively removing residual chemicals from the material by immersing it in a 5% NaClO solution, achieving transparent modification. Chen *et al*. (2023) successfully prepared a wood-like cellulose aerogel with both elasticity and conductivity using a 12% NaClO solution. Meanwhile, $NaClO_2$ has also been applied in the delignification process, and related research has been extensively conducted (Lin *et al*. 2019; Wu *et al.* 2019; Sun *et al*. 2023; Xu *et al*. 2023). Other alkaline solutions have also been used for the modification of wood-based materials, such as urea (Guo *et al*. 2022) and ammonia (Yin *et al*. 2022), which enrich the diversity of delignification technologies.

In summary, a plethora of research has been conducted both domestically and internationally on wood alkali treatment, primarily aiming to produce transparent wood, porous materials, and dense high-strength composite materials. Existing processes typically involve treatment durations exceeding 1.0 h and temperatures around 100 °C, posing challenges in terms of time and energy consumption during the alkali treatment stage. This study utilizes poplar wood as raw material and employs a coupling approach of NaOH solution treatment and thermal processing to produce glue-free self-adhesive laminated wood with superior bonding strength. This study integrates the alkali treatment and hot-pressing processes into a single step, which significantly reduces energy consumption and shortens the overall processing duration. Through microscopic structure observation and chemical composition analysis, the study explores the impact of the combined alkali treatment and hot-pressing process on the interfacial bonding characteristics of laminated wood, providing theoretical basis and technical support for the efficient and low-energy preparation of high-performance glue-free laminated wood.

EXPERIMENTAL

Materials

The poplar veneers had dimensions of 150 mm × 100 mm × 3 mm, a single-sheet weight of 45 g to 55.2 g, and a density ranging from 0.5 g/cm³ to 0.61 g/cm³. After oven-drying at 130 °C, the oven-dry weight of the specimens was measured, and the moisture content was 11.2%. It is calculated by dividing the mass of water present in wood by the mass of absolutely dry wood.

Chemically pure (CP) sodium hydroxide (NaOH) with a purity of 99.5% was supplied by Shanghai Aladdin Biochemical Technology Co., Ltd. (China). Three NaOH solutions with mass concentrations of 1%, 3%, and 5% were prepared by dissolving 1 g, 3 g, and 5 g of NaOH in 100 g of solution, respectively. Each mixture was stirred at 1000 rpm for 5 min until a clear solution was obtained.

Test Specimens

Specimens were fabricated by two hot-pressing layers of poplar wood without any adhesive. A 90 g/m² NaOH solution was swelled on the lower surface of the upper poplar layer (Fig. 1), and the specimens were prepared under controlled hot-pressing temperature and time.

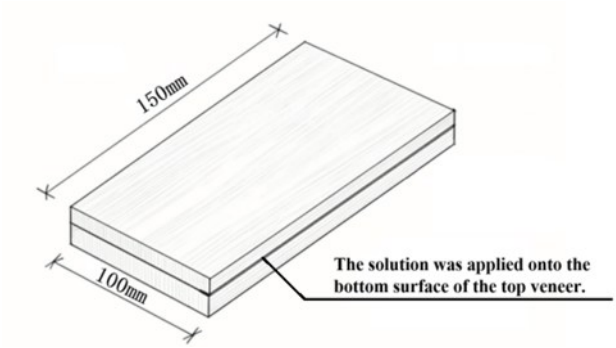

Fig. 1. Schematic diagram of veneer laminates and solution application

A Yisite laboratory-scale plate vulcanizing press was adopted as the hot-pressing equipment (Fig. 2). First, the specimens were hot-pressed at a temperature of 100 ℃ and a pressure of 6 MPa for 5 min. Subsequently, the temperature was raised to the target experimental temperatures of 120 ℃, 140 ℃, and 160 ℃, with the pressure maintained at 15 MPa for the corresponding durations of 30 min, 60 min, and 90 min, respectively. Upon reaching the preset holding time, the heat source was turned off, and the pressure was maintained for an additional 10 min. After that, the specimens were demolded and then subjected to cold pressing under a constant pressure for 1 to 2 days. Subsequently, the specimens should be machined to the corresponding dimensions (Fig. 3).

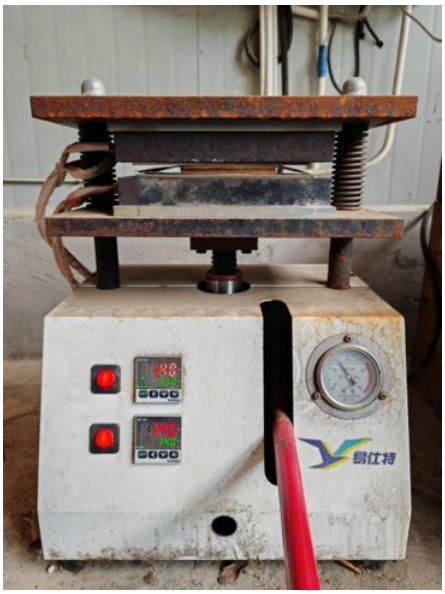

Fig. 2. Hot pressing process of wood veneers

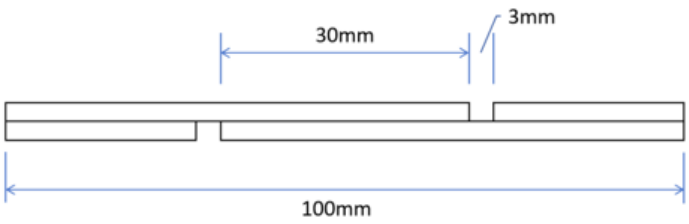

Fig. 3. Schematic diagram of slotting on wood veneers

Shear Bearing Capacity Test

Shear bearing capacity was tested using a universal testing machine (Fig. 4, WDW-300E, Jinan Popwil, Jinan, China). Both ends of the specimen were clamped (Fig. 5), and the specimen was fractured by downward movement of the crosshead. An orthogonal experiment was designed with three factors (hot pressing time, hot pressing temperature and concentration), each set at three levels. Five independent specimens were prepared using the same process and tested under identical environmental conditions.

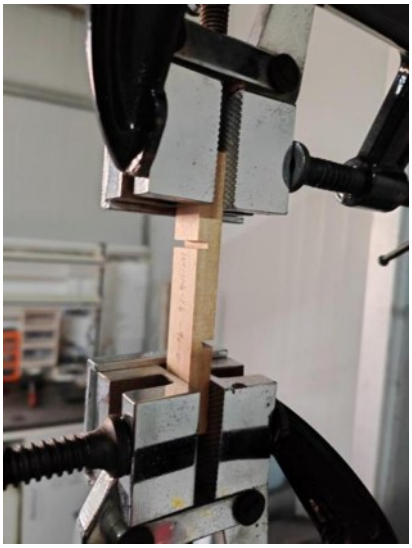

Fig. 4. Shear bearing capacity test of specimens

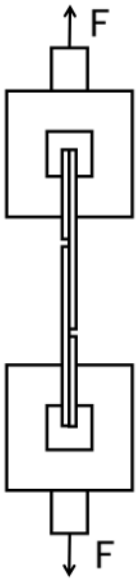

Fig. 5. Schematic diagram of shear bearing capacity test for specimens

Scanning Electron Microscopy

The sample was mounted directly onto conductive adhesive tape and sputter-coated with gold for 45 s using an SC7620 sputter coater (Quorum Technologies, UK) operated at 10 mA. Morphological imaging and energy-dispersive X-ray spectroscopy (EDS) elemental mapping were conducted using a Sigma 300 scanning electron microscope

(ZEISS, Germany). The morphological imaging was conducted at an acceleration voltage of 3 kV using the secondary electron (SE2) detector. Meanwhile, for the EDS elemental mapping, the acceleration voltage was set to 15 kV, and the same detector was employed.

Fourier transform infrared spectroscopy (FT-IR)

FT-IR spectra were obtained using a Nicolet iS20 FT-IR spectrometer (Thermo Fisher Scientific, USA), covering a spectral range of 4000 to 400 cm^{-1}. Each spectrum was recorded as an average of 32 scans with a resolution of 4 cm^{-1}. Before analysis, samples were ground into a fine powder, mixed with potassium bromide (KBr), and compressed into thin sheets.

RESULTS AND DISCUSSION

The Properties of the Specimens

Table 1. Properties of Specimens with Different Parameters

No.	Temperature (℃)	Concentration (%)	Time (min)	Shear Strength (MPa)
1	120	1	30	2.22 (0.51)
2	120	3	60	2.96 (0.78)
3	120	5	90	4.05 (0.72)
4	140	1	60	4.42 (0.23)
5	140	3	90	3.28 (0.54)
6	140	5	30	3.72 (0.37)
7	160	1	90	3.04 (0.51)
8	160	3	30	3.45 (0.61)
9	160	5	60	3.16 (0.68)
10	140	5	60	4.87 (0.56)

Values in parentheses are standard deviations

Table 2. Mean Values of Each Level for the Same Factor

Temperature (ºC)	Shear Strength (MPa)	Concentration (%)	Shear Strength (MPa)	Time (min)	Shear Strength (MPa)
120	3.08	1	3.23	30	3.13
140	3.81	3	3.23	60	3.51
160	3.22	5	3.64	90	3.46

Table 1 presents the statistical summary of shear strength for specimens prepared under 10 different process parameter combinations. Based on the data in Table 1, the average shear strength corresponding to each level of the process parameters can be calculated. As can be seen from Table 2, within the hot-pressing temperature range of 120 to 160 ℃, the shear strength first increased and then decreased with the rise of temperature. The shear strength of the specimens reached the maximum at a hot-pressing temperature of 140 ℃, which was 23.7% and 18.3% higher than that at 120 ℃ and 160 ℃, respectively. The concentration of NaOH solution also exerted a certain influence on the shear strength. Within the scope of this experiment, the shear strength of specimens treated with 1% and

3% NaOH solution was comparable, while that of specimens treated with 5% NaOH solution was the highest, which was 12.7% higher strength than those treated with the other two concentrations. The effect of hot-pressing time on the shear strength of specimens was consistent with that of hot pressing temperature, also showing a trend of first increasing and then decreasing. The shear strength of specimens treated with 60 min hot pressing was 12.1% and 1.4% higher than those treated with 30 min and 90 min hot pressing, respectively. In summary, the optimal parameters under the present experimental conditions were hot-pressing temperature of 140 ℃, NaOH concentration of 5%, and hot-pressing time of 60 min. The shear strength of the optimal parameter group reached 4.87 MPa, which was higher than the 4.44 MPa from Meng *et al*. (2023). Through observation of the failure modes of all specimens, it was found that all specimens failed at the bonding interface. Most of them exhibited interfacial failure as shown in Fig. 6(a) without obvious wood failure. Some specimens in Group 4 and the optimal group showed end wood failure, as illustrated in Fig. 6(b).

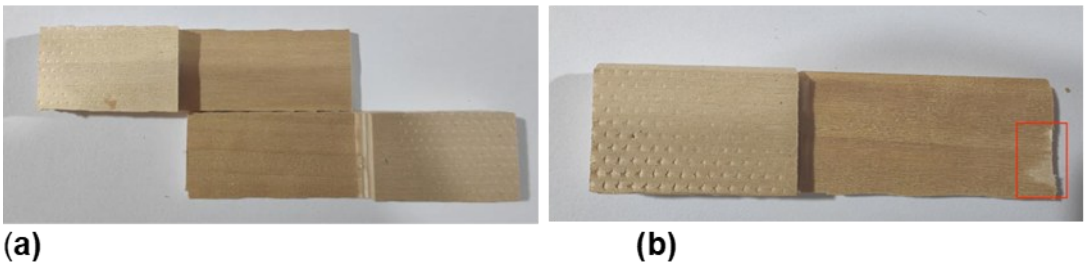

Fig. 6. Specimens failed at the bonding interface (a) no obvious wood failure observed; and (b) obvious wood failure occurred at the end

Analysis of Variance (ANOVA)

Shear strength was set as T. With the difference of specimen number, relative shear strength was T_i, The standard deviation was set as S_i. Temperature was taken as Factor A, with three levels, such as A1=120 ℃, A2=140 ℃, A3=160 ℃. Concentration was taken as Factor B, with three levels, such as B1=1%, B2=3%, B3=5%. Time was taken as Factor C, with three levels, such as C1=30 min, C2=60 min, C3=90 min. The sum of squares (SS), degrees of freedom (df), and mean square (MS) are listed in Table 3.

Table 3. ANOVA for Shear Strength

Source of Variation	SS	df	MS	F-value	$F_{0.05}$	$F_{0.01}$	Significance
A	4.503	2	2.252	6.84	3.26	5.26	Highly
B	1.722	2	0.861	2.62	3.26	5.26	No
C	1.284	2	0.642	1.95	3.26	5.26	No
Within-group error	11.852	36	0.329				
Total	28.579	44					

Thus, the temperature had a highly significant effect on shear strength, while concentration and time showed no significant effect. And then the post-hoc multiple comparisons were calculated by least significant difference (LSD).

$$LSD_{0.05}=t_{0.05/2,36}\times\sqrt{\frac{2MS_e}{3\times n}}=2.028\times\sqrt{\frac{2\times 0.329}{15}}=0.425$$

$$LSD_{0.01}=t_{0.005/2,36}\times\sqrt{\frac{2MS_e}{3\times n}}=2.719\times\sqrt{\frac{2\times 0.329}{15}}=0.570$$

A_2-A_1=3.81-3.08=0.73>0.57 (highly significant)
A_2-A_3=3.81-3.22=0.59>0.57 (highly significant)
A_3-A_1=3.22-3.08=0.14<0.425 (no significant)

Analysis of variance showed that temperature had a highly significant effect on shear strength. LSD post-hoc test further revealed that the shear strength at 140 ℃ was significantly higher than that at 12 a nd 160 ℃, while there was no significant difference between 120 and 160 ℃.

Analysis Using SEM

As can be seen from Fig. 7, the red rectangular box marks the adhesive boundary. In this region, various pores such as wood vessels have almost disappeared, forming a dense adhesive layer (Zhu *et al*. 2025). In areas away from the adhesive boundary, numerous incompletely crushed or compacted pores, as marked by the red ellipses, can still be observed. Figure 8 also shows that the effect of NaOH solution swelling is mainly concentrated near the adhesive boundary and has little influence on regions farther away from it. Figure 9 reveals that obvious sheared fibers exist at the bonding interface, and distinct molten lignin acts as an adhesive to bond fibers and form an adhesive layer throughout the entire bonding interface.

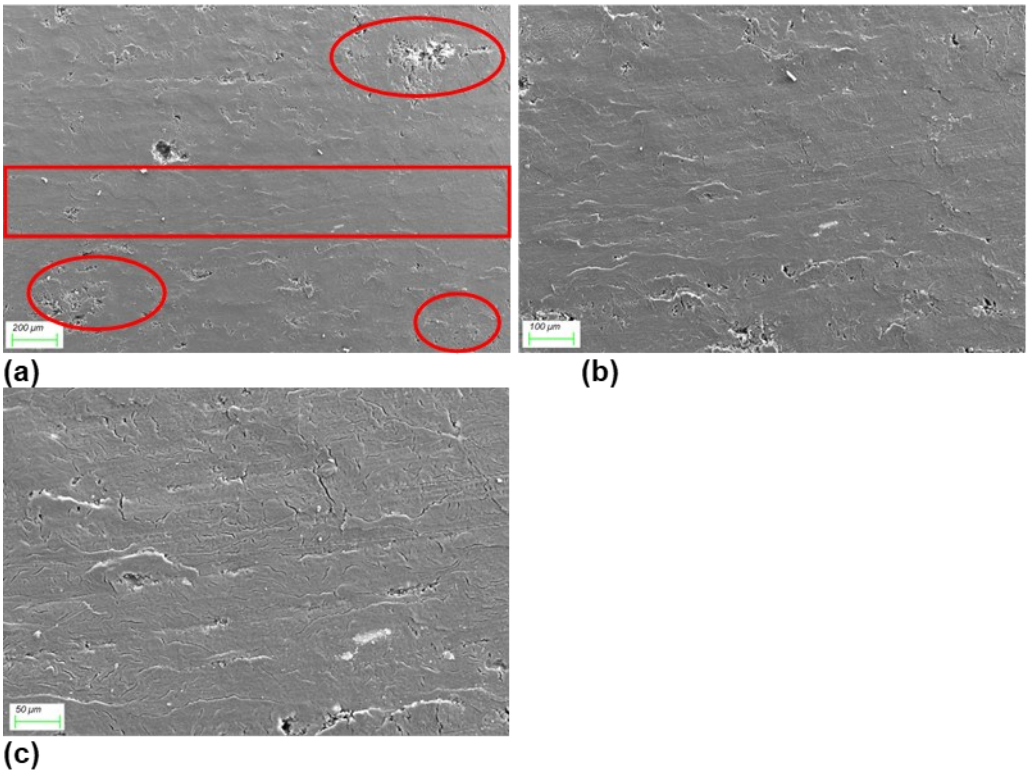

Fig. 7. Cross-sectional morphology magnified (a) 50, (b) 100 and (c) 200 times of group 10 specimens

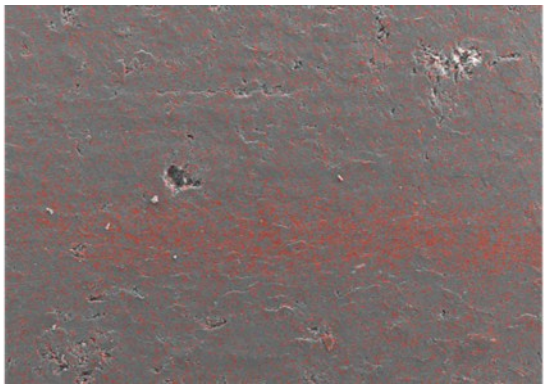

Fig. 8. The result of Na elemental mapping conducted on the bonding layer of Fig. 7(a)

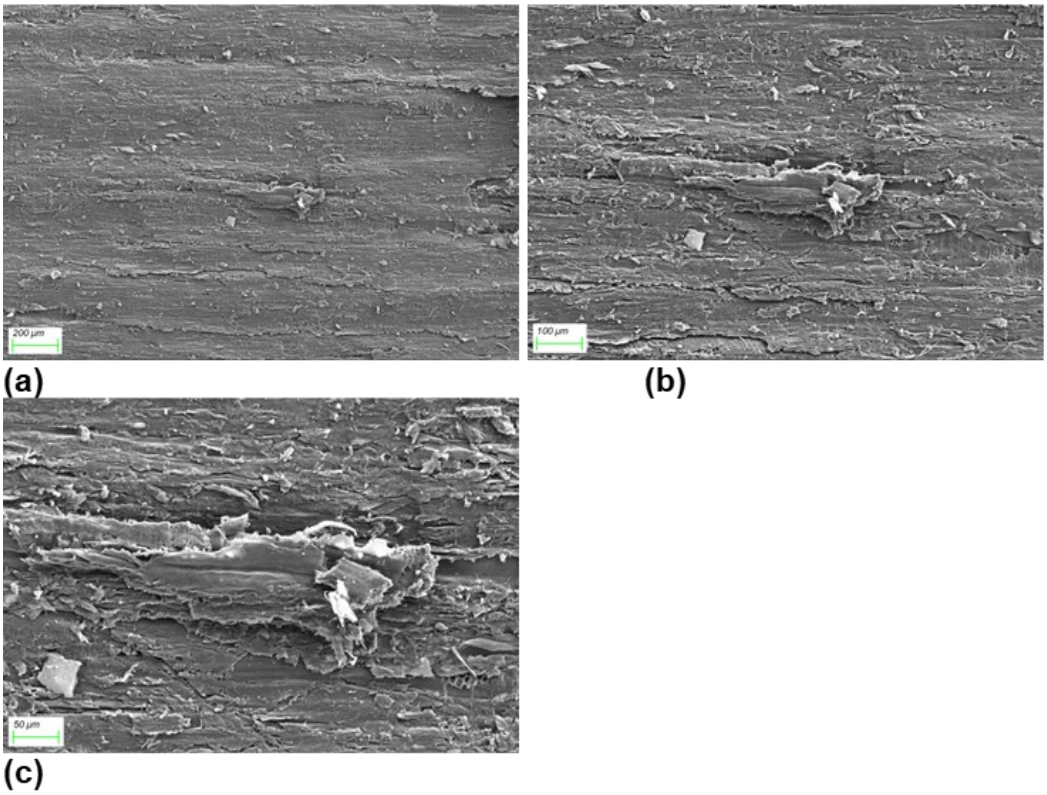

Fig. 9. Tangential morphology magnified (a) 50, (b) 100 and (c) 200 times of group 10 specimens

FT-IR Analysis

As shown in Figure 10, compared with natural wood, the bonding interface formed by hot pressing after alkali solution treatment showed varying degrees of reduction in the intensity of several absorption peaks. The peak at 1735 cm^{-1}, corresponding to the C=O stretching vibration of acetyl groups in hemicellulose, decreased significantly at the bonding surface. The peak at 1245 cm^{-1}, attributed to the C–O–C stretching vibration of ester linkages in hemicellulose, was also markedly weakened (Lian *et al*. 2024). These changes indicate that hemicellulose at the bonding surface had undergone substantial degradation under the process parameters described in this study.

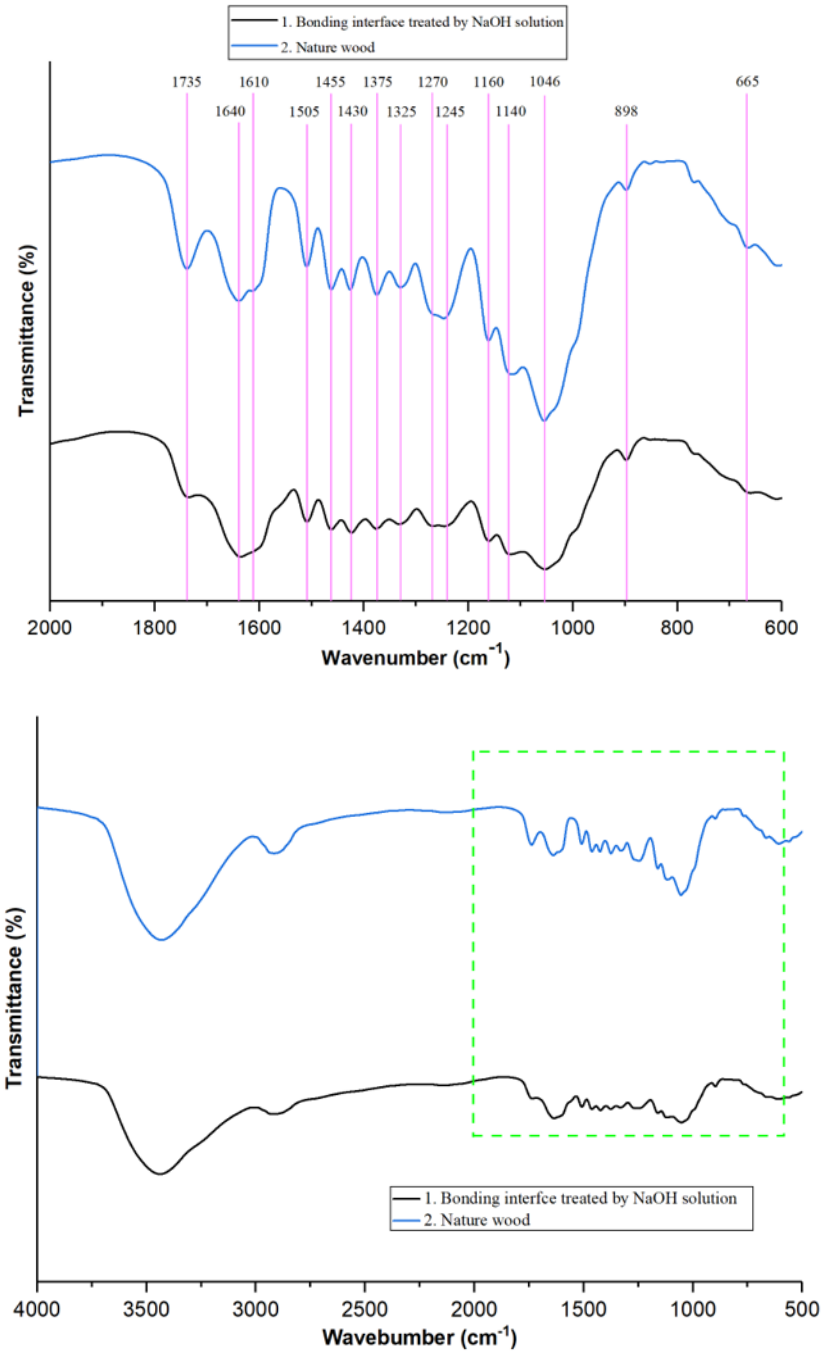

Fig. 10. FT-IR spectra of natural wood and bonding interface from group 10

The peak at 1375 cm^{-1} corresponds to the C–H bending vibrations of methylene (–CH_2–) and methyl (–CH_3) groups in cellulose and hemicellulose (Chen *et al*. 2011). The peak at 1430 cm^{-1} is ascribed to the C–H bending vibrations of methylene and methyl groups in cellulose and lignin; and the peak at 2900 cm^{-1} arises from the C–H stretching vibrations of methylene and methyl groups in cellulose and hemicellulose. The above variations demonstrate that the synergistic effect of sodium hydroxide and high temperature led to partial degradation of the molecular chains and amorphous regions of cellulose and hemicellulose.

The intensity of some characteristic peaks only showed minor fluctuations. The peak at 665 cm^{-1} corresponding to the out-of-plane bending vibrations of benzene rings in lignin, the peak at 1325 cm^{-1} associated with guaiacyl and syringyl ring vibrations in lignin, as well as the peak at 1455 cm^{-1} representing the skeletal vibrations of lignin aromatic rings, all exhibited slight intensity variations (Song *et al*. 2018). These results suggest that the primary structure of lignin was largely preserved without extensive degradation, despite certain impacts from the treatment.

CONCLUSIONS

1. Within the scope of this study, the optimal process parameters were determined as follows: Poplar wood surfaces were swelled with 5% sodium hydroxide solution, followed by hot-pressing at 140 °C for 60 min. The resulting shear strength of the bonding interface of the prepared specimens reached 4.87 MPa.
2. Analysis of variance revealed that the hot-pressing temperature had a highly significant effect on the shear strength of the bonding interface of the specimens.
3. Scanning electron microscopic analysis of the bonding interface and the adhesive boundary indicated that NaOH treatment exerted a significant effect at the boundary, where a dense adhesive layer was formed. Moreover, obvious molten lignin encapsulation of fibers was observed throughout the entire bonding interface. It can be seen from the FT-IR analysis that hemicellulose undergoes substantial degradation, while no significant degradation is observed in the skeletal structure of lignin.
4. In this study, specimens were prepared by directly swelling NaOH on wood surfaces followed by hot pressing. This process featured simple procedures and convenient operation. As alkali treatment and hot pressing were conducted simultaneously, which means that processing time and energy consumption were effectively reduced. Referring to relevant previous studies, this paper only took bonding strength as the core evaluation indicator to determine the optimal process parameters. Building on the optimal parameters obtained, subsequent work will further analyze other mechanical properties and also explore the application of interfacial coupling agents.

ACKNOWLEDGMENTS

The authors are grateful for the support of the Natural Science Foundation of the High Education Institutions of Jiangsu Province (Grant No. 22KJA220003).

REFERENCES CITED

Andze, L., Nefjodovs, V., Zoldners, J., Milbreta, U., Skute, M., Vecbiskena, L., Filipova, I., and Andzs, M. (2026). "NaOH-only pretreated wood densification: A simplified sulfite-free route across wood species," *Polymers* 18(3), article 312. https://doi.org/10.3390/polym18030312

Bay, M. S., Karimi, K., Esfahany, M. N., and Kumar, R. (2020). "Structural modification of pine and poplar wood by alkali pretreatment to improve ethanol production," *Industrial Crops and Products* 152, article 112506. https://doi.org/10.1016/j.indcrop.2020.112506

Chen, C. J., Song, J. W., Zhu, S. Z., Li, Y. J., Kuang, Y. D., Wan, J. Y., Kirsch, D. L., Xu, L. S., Wang, Y. B., Gao, T. T., Wang, Y. L., Huang, H., Gan, W. T., Gong, A., Li, T., Xie, J., and Hu, L. B. (2018). "Scalable and sustainable approach toward highly compressible, anisotropic, lamellar carbon sponge," *Chem* 4(3), 1-11. https://doi.org/10.1016/j.chempr.2017.12.028

Chen, F. B., Liao, Y., Wei, S., Zhou, H., Wu, Y., Qing, Y., Li, L., Luo, S., Tian, G. H., and Wu, Y. Q. (2023). "Wood-inspired elastic and conductive cellulose aerogel with anisotropic tubular and multilayered structure for wearable pressure sensors and supercapacitors," *International Journal of Biological Macromolecules* 250, article 126197. http://doi.org/10.1016/j.ijbiomac.2023.126197

Chen, W. H., and Kuo, P. C. (2011). "Isothermal torrefaction kinetics of hemicellulose, cellulose, lignin and xylan using thermogravimetric analysis," *Energy* 36(11), 6451-6460. http://doi.org/10.1016/j.energy.2011.09.022

Fan, H. Y., Chen, L. H., Miao, Q. X., Huang, L. L., and Zhou, X. X. (2020). "Preparation and characterization of natural moso bamboo fiber," *Forestry Machinery and Wood working Equipment* 48(5), 37-41. http://doi.org/10.13279/j.cnki.fmwe.2020.0056

Guo, Z. X., Wang, H., Di, M. W., and Zhao, J. N. (2022). "Freezing activation of wood fibers and preparation of binder-free boards," *Biomass Chemical Engineering* 56(3), 16-22. http://doi.org/10.3969/j.issn.1673-5854.2022.03.003

Hu, J., Wu, J. Y., Huang, Y. X., He, Y. Q., Lin, J., Zhang, Y. M., Zhang, Y. H., Yu, Y. L., and Yu, W. J. (2023). "Super-strong biomimetic bulk bamboo-based composites by a neural network interfacial design strategy," *Chemical Engineering Journal* 475, article 146435. http://doi.org/10.1016/j.cej.2023.146435

Jungstedt, E., Montanari, C., Ostlund, S., and Berglund, L. (2020). "Mechanical properties of transparent high strength biocomposites from delignified wood veneer," *Composites Part A: Applied Science and Manufacturing* 2020, 105853. http://doi.org/10.1016/j.compositesa.2020.105853

Lian, H. Y., Li, P. S., Xu, Y. T., Zhang, X. C. (2024). "A simple and sustainable method for preparing high-strength, lightweight, dimensional stable, and mildew resistant multifunctional bamboo," *Construction and Building Materials* 415, article 135027. http://doi.org/10.1016/j.conbuildmat.2024.135027

Lin, T., Fan, J., Yin, X. F., Tian, X. H., and Wang, Z. X. (2019). "Process in preparation of transparent wood composites," *Modern Chemical Industry* 39(8), 43-48. http://doi.org/10.16606/j.cnki.issn.0253-4320.2019.08.009

Liu, Y. D. (2025). *Study on Dyeing and Properties of Poplar Veneer Imitating Precious Wood Based on Deep Eutectic Solvent Treatment*, Doctor's Thesis, Northeast Forestry University. Heilongjiang, China.

Meng, T. T., Ding, Y., Liu, Y., Xu, L., Mao, Y. M., Gelfond, J., Li, S. K., Li, Z. H., Salipante, P. F., Kim, H., Zhu, J. Y., Pan, X. J., and Hu, L. B. (2023). "In situ lignin adhesion for high-performance bamboo composites," *Nano Letters* 23, 8411-8418. http://doi.org/10.1021/acs.nanolett.3c01497

Mi, R. Y., Li, T., Dalgo, D., Chen, C. J., Kuang, Y. D., He, S. M., Zhao, X. P., Xie, W. Q., Gan, W. T., Zhu, J. Y., *et al*. (2019). "A clear, strong, and thermally insulated

transparent wood for energy efficient windows," *Advanced Functional Materials* 2019, article 1907511. http://doi.org/10.1002/adfm.201907511

Pang, X. N., Yang, X., Li, X. J., Cao, M., and Yang, X. (2021). "Improvement of porosity and dye permeability of moso bamboo splints by alkali etching," *Journal of Forestry Engineering* 6(6), 44-50. http://doi.org/10.13360/j.issn.2096-1359.202012030

Qi, Y. Q., Zhou, Z. W., Xu, R., Dong, Y. T., Zhang, Z. Q., and Liu, M. J. (2023). "Effect of NaOH pretreatment on permeability and surface properties of three wood species," *ACS Omega* 8(43), article 3c04745. http://doi.org/10.1021/acsomega.3c04745

Qian, J., Yue, K., Liu, S. D., Lu, D., Wu, P., and Li, Q. (2024). "Augmenting bamboo strength and thermal stability for sustainable construction," *Journal of Cleaner Production* 451, article 142073. http://doi.org/10.1016/j.jclepro.2024.142073

Qiu, F. (2025). *The Preparation of Wood-based Silver Nanowire Composites and their Electromagnetic Shielding Performance Study*, Master's Thesis, Guangxi University, Guangxi, China.

Song, J. W., Chen, C. J., Zhu, S. Z., Zhu, M. W., Dai, J. Q., Ray, U., Li, Y. J., Kuang, Y. D., Li, Y. F., Quispe, N., *et al*. (2018). "Processing bulk natural wood into a high-performance structural material," *Nature* 554, 224-228. http://doi.org/10.1038/nature25476

Sun, H., Gong, Y. Z., Yan, Y. T., Li, S., Fu, C. Q., Chang, X., and Chen, T. A. (2023). "Effect of delignification on cell wall structure of fast-growing poplar and Chinese fir," *Journal of Forestry Engineering* 8(5), 46-54. http://doi.org/10.13360/j.issn.2096-1359.202210009

Wang, W. J., Zhang, J., Zhang, Y. X., He, L., and Xie, X. Y. (2025). "Properties and water purification efficacy of alkali-modified balsam wood filler," *Technology of Water Treatment* 51(07), 97-104. http://doi.org/10.16796/j.cnki.1000-3770.2025.07.016

Wang, X., Guan, H., Dai, X. J., Ni, L., and Wang, X. Q. (2023). "Research process of wood/metal-organic frameworks composites," *Chinese Journal of Wood Science and Technology* 37(1), 8-17. http://doi.org/10.12326/j.2096-9694.2022205

Wu, Y., Han, Y., Huang, N., Wu, J. M., Tang, C. Y., Zhou, J. C., and Huang, Q. T. (2019). "Effect of delignification process on properties of transparent wood," *Journal of Forestry Engineering* 4(6), 98-104. http://doi.org/10.13360/j.issn.2096-1359.2019.06.014

Wu, Y., Zhou, J. C., Huang, Q. T., Yang, F., Wang, Y. J., Liang, X. M., and Li, J. Z. (2020). "Study on the colorimetry properties of transparent wood prepared from six wood species," *ACS Omega* 5, 1782-1788. http://doi.org/10.1021/acsomega.9b02498

Xu, L. L., Xiong, Y., Dang, B. K., Ye, Z. N., Jin, C. D., Sun, Q. F., and Yu, X. H. (2019). "In-situ anchoring of Fe_3O_4-ZIF-67 dodecahedrons in highly compressible wood aerogel with excellent microwave absorption properties," *Materials and Design* 182, article 108006. http://doi.org/10.1016/j.matdes.2019.108006

Xu, W., and Zhou, J. C. (2023). "Fundamental research and application progress of transparent wood interface," *Journal of Forestry Engineering* 8(2), 1-9. http://doi.org/10.13360/j.issn.2096-1359.202112003

Yang, R., Cao, Q. H., Mei, C. T., Hong, S., Xu, Z., and Li, J. Z. (2020). "Research process of functional composite materials constructed from high porosity three-dimensional structural wood," *Acta Materials Compositae Sinica* 37, article 1. http://doi.org/10.13801/j.cnki.fhclxb.20200324.001

Yang, Y. S., Dang, B. K., Wang, C., Chen, Y. P., Chen, K. C., Chen, X. J., Li, Y. Y., and Sun, Q. F. (2023). "Anisotropic nature of lightweight wooden metamaterials with mechanical thermomechanical multistability," *Advanced Functional Materials* 2023, article 2307242. http://doi.org/10.1002/adfm.202307242

Ye, H. R., Shi, Y., Xu, B. B., Guo, Z. H., Fan, W., Zhang, Z. F., Mulvihill, D. M., Zhang, X. H., Shi, P. J., He, X. M., and Ge, S. B. (2023). "Sustainable ultra-strong thermally conductive wood-based antibacterial structural materials with anti-corrosion and ultraviolet shielding," *EcoMat* 2023, article e12420. http://doi.org/10.1002/eom2.12420

Yin, B., Du, W. X., Zhang, Y., Gao, X., Ma, C., and Guo, M. H. (2022). "Preparation and photocatalytic performance of biomimetic wood structure cerium vanadate," *Journal of Forestry Engineering* 7(4), 38-45. http://doi.org/10.13360/j.issn.2096-1359.202111037

Zhao, H., Miao, Q. X., Huang, L. L., Zhou, X. X., and Chen, L. H. (2021). "Preparation of long bamboo fiber and its reinforced polypropylene membrane composites," *Journal of Forestry Engineering* 6(5), 96-103. http://doi.org/10.13360/j.issn.2096-1359.202101020

Zheng, X. R., and Qin, Y. L. (2025). "Study on improving the permeability of eucalyptus urophylla with a mixed solution of NaOH and Na_2SO_3," *China Forest Products Industry* 62(07), 47-51. http://doi.org/10.19531/j.issn1001-5299.202507008

Zhu, X. D., Xue, Y. Y., Qian, L., Mei, C. T., and Gao, Y. (2025). "Fabrication of self-bonding laminated bamboo via a dual-treatment method combining alkali treatment and hot pressing," *Construction and Building Materials* 490(5), article 142553. http://doi.org/10.1016/j.conbuildmat.2025.142553

Article submitted: April 14, 2026; Peer review completed: May 25, 2026; Revised version received: July 24, 2026; Accepted: July 25, 2026; Published: August 10, 2026.
DOI: 10.15376/biores.21.4.9541-9554